

Available online at [www.sciencedirect.com](http://www.sciencedirect.com)

ScienceDirect

Biomedical Journal

journal homepage: [www.elsevier.com/locate/bj](http://www.elsevier.com/locate/bj)

## Review Article

# Clinical applications of spectral domain optical coherence tomography in retinal diseases



R.K. Murthy, Shamim Haji, Kumar Sambhav, Sandeep Grover,  
K.V. Chalam\*

Department of Ophthalmology, University of Florida College of Medicine, Jacksonville, FL, USA



Prof. K.V. Chalam

## ARTICLE INFO

## Article history:

Received 17 December 2014

Accepted 20 July 2015

Available online 20 June 2016

## Keywords:

Macula

Retinal disorders

Optical coherence tomography

Spectral-domain optical coherence tomography

## ABSTRACT

Optical coherence tomography (OCT) was introduced about two decades ago and has revolutionized ophthalmic practice in recent years. It is a noninvasive noncontact imaging modality that provides a high-resolution cross-sectional image of the cornea, retina, choroid and optic nerve head, analogous to that of the histological section. Advances in OCT technology in signal detection technique from time-domain (TD) to spectral-domain (SD) detection have given us the potential to study various retinal layers more precisely and in less time. SD-OCT better delineates structural changes and fine lesions in the individual retinal layers. Thus, we have gained substantial information about the pathologic and structural changes in ocular conditions with primary or secondary retinal involvement. This review we discuss the clinical application of currently available SD-OCT in various retinal pathologies. Furthermore, highlights the benefits of SD-OCT over TD. With the introduction of enhanced depth imaging and swept – source OCT visualization of the choroid and choriocapillaris has become possible. Therefore, OCT has become an indispensable ancillary test in the diagnosis and management of diseases involving the retina and/or the choroid. As OCT technology continues to develop further it will provide new insights into the retinal and choroidal structure and the pathogenesis of posterior segment of the eye.

Optical coherence tomography (OCT) has emerged as an important imaging modality in the evaluation and management of retinal disease. The noninvasive nature of the test and the ability to image intra-ocular structures *in vivo* with resolution approaching that of histological sections has made OCT particularly useful in the detection and quantification of

macular and optic nerve head pathologies [1–5]. Since its introduction in the late 1990s for clinical application in the imaging of retinal and optic nerve disorders, OCT has shown major improvements in technology with increasing resolution of the images.

\* Corresponding author. Department of Ophthalmology, University of Florida College of Medicine, 580 W 8th Street, Tower 2, 3rd Floor, Jacksonville, FL 32209, USA. Tel.: +1 904 2449361; fax: +1 904 2449391.

E-mail address: [kvchalam@aol.com](mailto:kvchalam@aol.com) (K.V. Chalam).

Peer review under responsibility of Chang Gung University.

<http://dx.doi.org/10.1016/j.bj.2016.04.003>

2319-4170/© 2016 Chang Gung University. Publishing services by Elsevier B.V. This is an open access article under the CC BY-NC-ND license (<http://creativecommons.org/licenses/by-nc-nd/4.0/>).

First reported in 1991, OCT is analogous to ultrasonic pulse-echo imaging, but instead of sound waves, it uses near-infrared light to produce cross-sectional or three-dimensional (3D) images of the retina [1–8]. The images are generated through the measurement of magnitude and echo time delay of back scattered light from an optical beam across the retina. Since direct detection of light echoes is not possible due to the high velocity of light, measurements are done correlating sample reflections from a reference mirror using a Michelson interferometer. In this arrangement of the system, referred to as the time-domain (TD) OCT, one arm of the interferometer directs lights and collects the back scattered signal from the object of interest. A second reference arm with a reflecting mirror is mechanically controlled to vary the time delay and measure interference. The combination of reflected light from the sample arm and reference light from the reference arm gives rise to an interference pattern, given that light from both arms has traveled similar optical distance within the coherence length. Areas of the sample that reflect back a lot of light will create greater interference than areas that do not. Any light that is outside the short coherence length will not interfere. This reflectivity profile, called an A-scan contains information about the spatial dimensions and location of structures within the item of interest. A cross-sectional tomographic B-scan is achieved by laterally combining a series of A-scans.

However, conventional TD-OCT has several limitations. Because there is a time delay involved during the axial translation of the reference mirror, the number of A scans acquired is limited, resulting in a B-scan with poor resolution. Another related problem is the lack of registration, poor point to point correlation between an OCT B-scan and the patient's fundus. A final critical limitation related to the slow-speed of TD-OCT is poor sampling density. Large amount of data is interpolated by sampling only a fraction of the mapped area.

Within the past decade, a new generation of OCT technology known as “SD-OCT” or “Fourier domain” OCT has evolved. In SD-OCT, light echoes are detected by measuring the interference signal as a function of wavelength by the use of an interferometer with a stationary reference arm [9]. The measurement of light echoes simultaneously allows high speed scanning with scan rates 50–100 times faster than conventional TD-OCT. This results in improved resolution of the B-scan images (the axial resolution on SD-OCT is 4–7  $\mu$  as

compared to 10  $\mu$  on the Stratus TD-OCT) [6–8]. Spectralis (Heidelberg Engineering, Vista, CA/Germany), one of the commercially available SD-OCT, also incorporates the Tru-track™ technology, which significantly reduces image corruption due to motion artifacts and provides the opportunity to correlate quantitatively the same areas of retinal pathology at sequential time points [Fig. 1].

### Imaging on spectral-domain optical coherence tomography

Retinal cross-sectional imaging on Stratus OCT is dominated by signals from the nerve fiber layer (NFL), the outer segment-inner segment line of the photoreceptors (ellipsoid zone) and the retinal pigment epithelium (RPE). Low-backscattering ganglion cell layer (GCL), external limiting membrane (ELM) are poorly resolved as well as the boundaries between the transparent and highly scattering layers such as the NFL, the inner plexiform layer (IPL), the outer plexiform layer (OPL), the ellipsoid zone (also known as IS-OS line) and the RPE [Fig. 2].

The demonstrated improvement in speed with SD-OCT allows for a shift from two-dimensional sampling to comprehensive 3D screening of ocular pathology with OCT [9]. The ultrahigh resolution images enable excellent visualization of the architectural morphology of the internal retinal layers. Although the axial image resolutions are comparable in the SD and the TD-OCT images, the increase in the transverse pixel density which is possible using SD-OCT significantly improves the visualization of retinal architecture. In addition, intra-retinal interfaces are continuous in the higher transverse pixel density, SD ultrahigh-resolution OCT image [9]. On SD-OCT, the following bands are seen outside the hypo-reflective band of the outer nuclear layer (ONL) by SD-OCT at the fovea in healthy eyes: (1) A thin, hyper-reflective band presumably corresponding to the ELM; (2) a slightly thicker hyper-reflective band presumably corresponding to the interface of the inner and outer segments of the photoreceptor layer (PRL); (3) a thin, only occasionally visible, hyper-reflective band presumably corresponding to the outer segment-RPE interdigitation; and (4) a broad hyper-reflective band thought to correspond to the RPE/Bruch's membrane complex [Fig. 3].

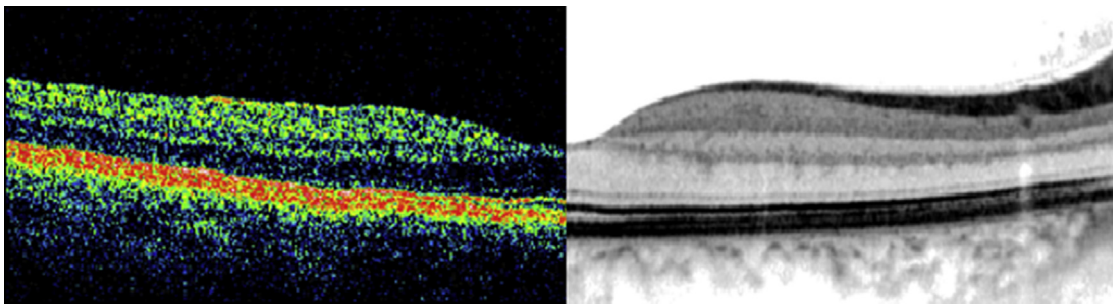


Fig. 1 – Retinal cross-sectional image from the same subject on time-domain Stratus optical coherence tomography (left) and spectral-domain Spectralis optical coherence tomography (right).

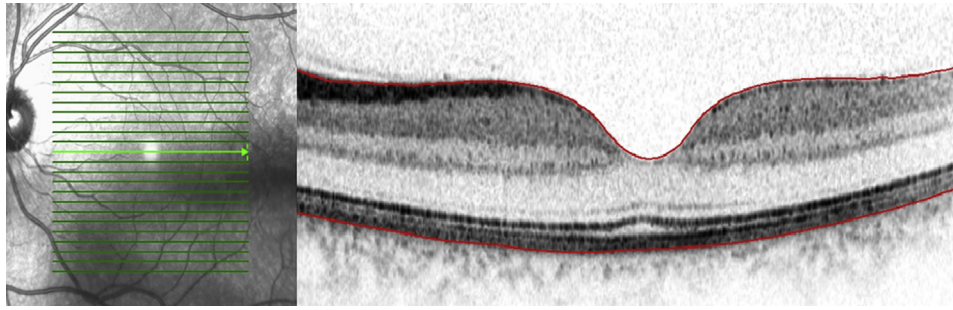


Fig. 2 – Cross-sectional Spectralis optical coherence tomography image of a normal subject revealing all the retinal layers. The red lines indicate the demarcation of the inner limiting layer (top) and the basement membrane of RPE-Bruch's membrane complex (bottom).

Another advantage of SD-OCT is improved retinal coverage by the scan protocols. The standard scan protocol on SD-OCT machines covers  $6\text{ mm} \times 6\text{ mm}$  surface of the retina, generating 21 B-scan images in 1.4 s, which is comparable to the

time required for a single Stratus OCT image. The vertical distance between consecutive images in the raster is  $300\ \mu\text{m}$ , which can be reduced to as low as  $50\ \mu\text{m}$  in some of the SD-OCT machines in contrast to the  $1.6\text{ mm}$  spacing on Stratus OCT macular mapping protocol. Increased density of scans has the potential to detect small focal changes in the parafoveal region that are not detectable by standard TD-OCT imaging protocol [8].

Han and Jaffe [10] have reported that in spite of the high-speed scanning ability and increased resolution of scans, SD-OCT images are not totally devoid of image artifacts. Among the artifacts are misidentification of the boundaries of the inner and outer retina, degraded scan image, off-center scans not properly centered on an identifiable foveal depression, and out-of-register artifacts in which the inner retina was truncated because of a superiorly shifted scan. Clinically significant artifacts involving the center 1-mm area were seen in 5.1% of cirrus and 8.0% of Spectralis OCT scans.

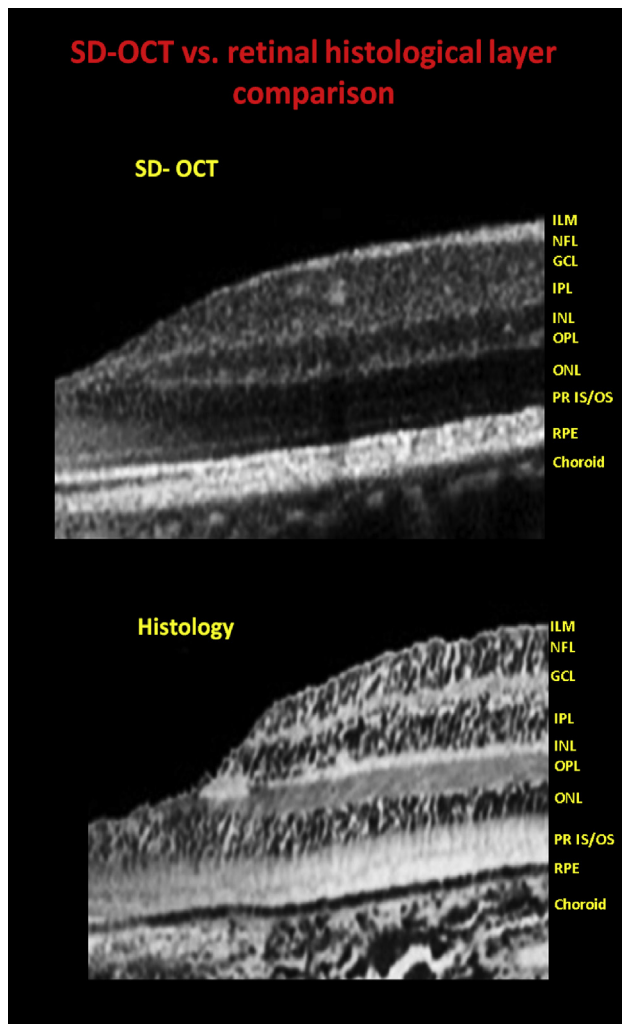


Fig. 3 – Cross-sectional foveal image of a normal subject on Spectralis optical coherence tomography with delineation of all the layers of the retina (top). Comparative histological section of the fovea of a normal human eye (bottom).

### Macular measurements on spectral-domain optical coherence tomography

Quantification of macular thickness by OCT in a reproducible, noninvasive way allows clinicians to monitor the efficacy of treatment for macular pathology like macular edema. Stratus OCT provides automated measurements of mean retinal thickness of the center point and each of four inner and four outer subfields (in micrometers), and total macular volume (in cubic millimeters). An average of all points within the inner circle of 1-mm diameter is defined as central foveal subfield (CSF) thickness [Fig. 4]. The OCT software identifies the center point as the intersection of six radial lines and reports the center point thickness as the average of the six measurements of thickness at the center point [8].

There are not only differences in measurement algorithms of macular thickness between TD and SD OCTs but also between OCT machines of the same generation produced by different manufacturers. Stratus TD-OCT measures retinal thickness between ILM and the ellipsoid zone of the photoreceptor. Cirrus SD-OCT measures macular thickness between ILM and RPE while Spectralis SD-OCT includes Bruch's membrane within the macular thickness [11]. That probably explains why the CSF

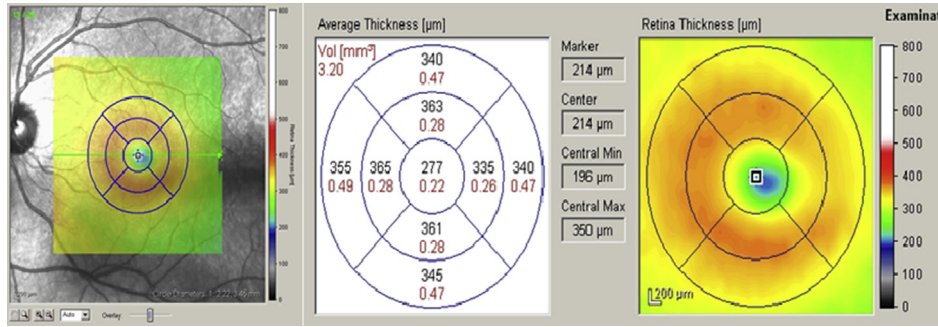


Fig. 4 – Spectralis optical coherence tomography showing of the left eye of a normal subject with macular thickness map overlay on the infrared image (left), retinal thickness and volume data for the nine ETDRS subfields (middle) and color map (right).

thickness on the Spectralis OCT is approximately 60  $\mu$  more when compared to that on Stratus OCT [12].

The reliability of change analysis of macular thickness correlates with the reproducibility of measurements on the OCT machines [13]. Numerous studies have confirmed the high reproducibility of macular thickness measurements in TD-OCT [14–17]. The Diabetic Retinopathy Clinical Research Network showed that total macular volume has better reproducibility in cases where there is diffuse macular edema. Studies done on SD-OCT systems have found higher reproducibility as compared to TD-OCT [18–20]. Leung et al. [19], have suggested that the higher reproducibility observed in SD-OCT systems compared with those in TD-OCT may be due to the higher scan rate of the former, which enables macular mapping with fewer motion artifacts and thus is more accurate and repeatable segmentation.

Studies have been done to understand how TD-OCT and SD-OCT data compare to each other in pathological retinal conditions, as both are frequently used to determine eligibility, treatment and outcome criteria in clinical trials and clinical practice. Forooghian et al. [21], have reported that although the two systems appear equally reliable in generating macular measurements, they may not be used interchangeably for clinical practice and research.

## Spectral-domain optical coherence tomography in retinal conditions

### Spectral-domain optical coherence tomography in diabetic macular edema

With the advent of OCT, classification of DME has moved from the traditional one based on angiographic leakage to the one defining structural changes seen in the retina. Otani and Kishi [22] described three OCT patterns of DME on Stratus OCT: simple sponge-like retinal swelling, cystoid macular edema (CME) and serous retinal detachment. With better delineation of different retinal layers on SD-OCT, more detailed *in vivo* histological changes occurring in DME have been reported. Leung et al. [19], in their study of 59 patients with DME reported a correlation with the severity of DME to location of cystic spaces using OPKO/OTI SD-OCT (OPKO-OTI, Miami, FL,

USA). For mild retinal edema on fluorescein angiography (FA), cystic spaces were located only in the OPL. When the cystic spaces became more pronounced or when they were ill-defined, they involved both the OPL and ONL. However, they did not find any significant correlation between the severity of cystic changes and the source (diffuse or focal) of fluorescein leakage [Fig. 5].

Macular thickness on OCT is often used as an outcome measure to assess the effects of various treatments on Diabetic Macular Edema (DME). However, correlation between OCT-measured macular thickness and visual acuity has been variable. Assessing the status of the ellipsoid zone on SD-OCT is a measure of the health of photoreceptors and has been shown to correlate with visual acuity in a number of retinal conditions. Maheshwary et al. [23], have quantified the percentage disruption of ellipsoid zone in patients with DME and report that it correlates directly with visual acuity. However, percentage measurement of disruption of ellipsoid zone is prone to measurement bias and search is on for a parameter on SD-OCT, which can act as a surrogate for visual acuity in these patients. One such parameter is the use of photoreceptor outer segment (PROS) length. Forooghian et al. [20], using segmentation algorithm on Cirrus SD-OCT have reported strong correlation of PROS length with visual acuity. However, segmentation algorithms to

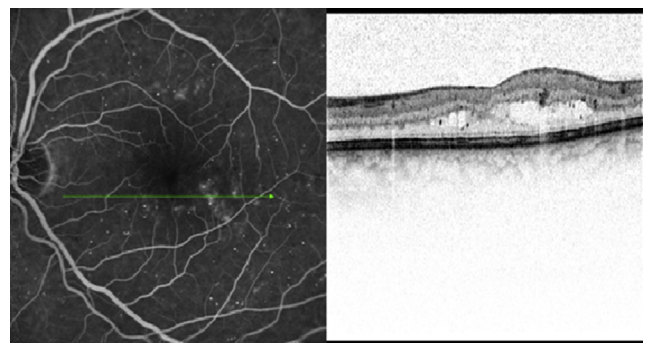


Fig. 5 – Cross-sectional line scan image on Spectralis optical coherence tomography showing cystic inner retinal swelling in patient with diabetic macular edema.

measure individual layers are still evolving and future studies on more SD-OCT machines in normal and pathological conditions are required before it can be used reliably in clinical practice.

### Spectral-domain optical coherence tomography in age-related macular degeneration

With the advent of high-resolution OCT imaging, new insights have been achieved in phenotypic variations of age-related macular degeneration (AMD). A wide range of alterations in the photoreceptor, RPE-Bruch's membrane–choriocapillaris complex are being described. In the nonexudative form of AMD, drusen are seen as dome-shaped elevations of the RPE band in SD-OCT with more elongated elevations consistent

with sub-RPE deposits [Fig. 6A]. Using Spectralis OCT, Querques et al. [24], have revealed that the hitherto less understood reticular drusen are actually subretinal drusenoid deposits and are distinct from the sub RPE deposits found in soft drusen.

Thinning or thickening of the RPE band in the OCT scan reflects boundaries of enlarged or attenuated RPE cells. Schuman et al. [25], in their study of 12 subjects with drusen using SD-OCT measured the PRL thickness in areas overlying drusen (size more than 125  $\mu$ ) and have reported that there was focal PRL thinning over drusen compared to age-matched controls, with drusen height having a much stronger correlation than drusen width with the extent of PRL thinning over drusen locations. Evaluation of drusen using SD-OCT is currently underway on a larger scale in the age-related Eye Disease Study 2 (AREDS-2) ancillary SD-OCT study, in high risk drusen eyes with annual follow-up of up to 5 years.

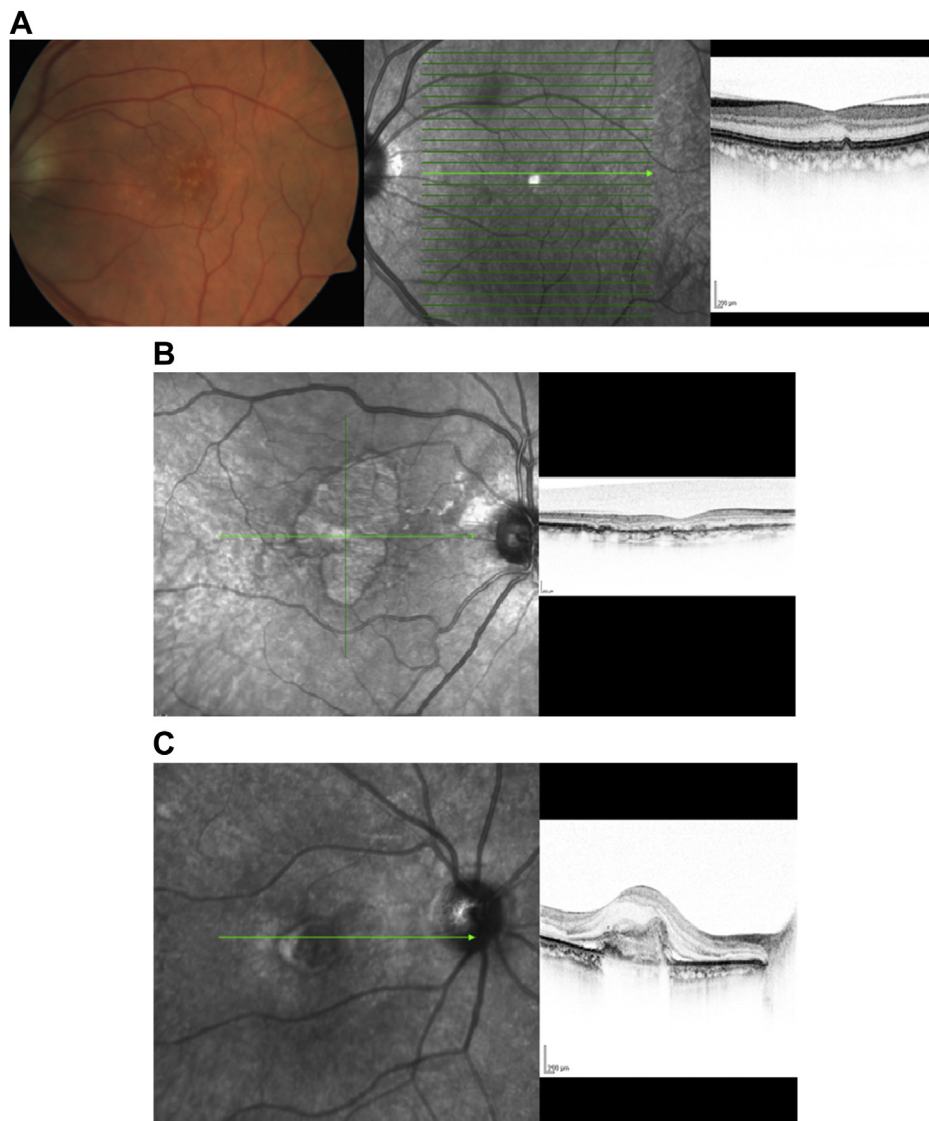


Fig. 6 – (A) Fundus photo and corresponding infrared image and cross-sectional line scan image on Spectralis optical coherence tomography of a patient with early age-related macular degeneration changes revealing drusen. (B) Cross-sectional Spectralis optical coherence tomography image of left eye of a patient with geographic atrophy showing outer retinal atrophy with RPE irregularity. (C) Cross-sectional Spectralis optical coherence tomography image of left eye of a patient with exudative age-related macular degeneration revealing choroidal neovascularization with overlying retinal edema and subretinal fluid.

In eyes with advanced AMD showing geographic atrophy [Fig. 6B], Fleckenstein et al. [26], have described the morphological patterns seen on SD-OCT by dividing them into three zones: perilesional, junctional, and atrophic zones. On Spectralis OCT, the perilesional zone reveals typical changes seen in early AMD including drusen and RPE changes. At the junctional zone, along with the above changes, there is loss of overlying photoreceptors for some distance beyond the edge or together with the RPE, with the ELM ending in a curved line. There is loss of ONL as well with an attenuated OPL resting directly on Bruch's membrane or the remaining sub-RPE deposits. Within the atrophic zone itself, islands with preserved layers (i.e., RPE-, IPL-band, ELM, ONL, and OPL) were noted. In another study by the same authors, swelling and widening of visible structures at the foveal ONL was seen on Spectralis OCT in patients with fovea spared geographic atrophy, which they hypothesized, is a reflection of a preapoptotic stage of neuronal cellular elements indicating imminent atrophy.

Margolis and Spaide [27], have proposed a novel enhanced depth imaging (EDI) technique of imaging the RPE-Bruch's--choriocapillaris complex using Spectralis OCT. This is done by positioning the scanner closer to the eye than the standard, such that a stable inverted image is produced, with better resolution of deeper layers, namely choroid. This new EDI technique provides new evidence that pigment epithelial detachments (PED), previously visualized as optically empty on Stratus OCT has some sort of internal structure along the back surface of the RPE. He proposes that this new evidence supports Gass' hypothesis that development of PED is associated with an underlying choroidal neovascular membrane.

In patients with exudative AMD, SD-OCT by its ability to yield high resolution 3D images, provides volumetric measurements of choroidal neovascular membrane and is more sensitive than Stratus OCT in identifying abnormalities such as subretinal fluid and retinal edema [Fig. 6C]. Khurana et al. [28], in their comparative study of FA, TD-OCT and SD-OCT findings in patient with CNV noted that SD-OCT picked up more than 90% of cases of CNV identified on FA compared to 59% on Stratus OCT. However, they cautioned that SD-OCT did not identify all cases with fluorescein leakage from CNV, and is accompanied by a decreased specificity, such that abnormalities might warrant consideration of retreatment (e.g., persistent cystoid abnormalities in the absence of fluorescein leakage from CNV). Framme et al. [29], evaluated morphological changes in CNV on SD-OCT after anti-VEGF monotherapy in patients with exudative AMD to see if anti-VEGF therapy caused CNV regression or stops further CNV growth. They found that there was no change in CNV morphology on SD-OCT after anti-VEGF treatment in over 80% of patients. Patients with classic CNV on fluorescein angiogram showed a small change in the overall thickness of CNV with no change in the diameter.

---

### **Spectral-domain optical coherence tomography in cystoid macular edema secondary to vein occlusion**

Imaging by OCT in CME due to retinal vein occlusions has given an insight into the pathology of the condition. On TD

Stratus OCT, the location of cysts could not be correlated to the corresponding layer in the retina and were grouped as outer, or inner retinal cyst. On SD-OCT, Ota et al. [30], observed that cysts in the fovea were located predominantly in the outer plexiform and inner nuclear layers, whereas in the extra-foveal area, small cystoid spaces were seen less frequently in the other retinal layers [Fig. 7A]. In addition, they reported that discontinuity in the ELM layer on the SD-OCT is a poor prognostic factor for visual outcome in these patients. This has been observed by SD-OCT in patients with other retinal pathologies, including AMD and DME.

In patients with long standing CME, in cases due to retinal vascular occlusion, a subfoveal sensory detachment is seen. The pathophysiology of the sensory detachment is unknown with underlying RPE pump disturbance due to ischemia suspected to be the likely cause [31]. Ota et al. [31], have produced new evidence on SD-OCT implicating tractional forces by the expanding Muller's cells on the photoreceptors as the likely etiology for the development of serous detachment [Fig. 7B].

---

### **Spectral-domain optical coherence tomography in plaquenil maculopathy**

One of the novel applications of SD-OCT has been to identify subclinical damage in the photoreceptors in patients on chronic use of hydroxychloroquine. Chen et al. [32] first reported abnormalities in the perifoveal photoreceptor ellipsoid zone were seen on SD-OCT in asymptomatic patients on hydroxychloroquine. In patients who are asymptomatic, Chen et al. [32], have reported that thinning of GCL and retinal NFL precedes the involvement of outer retina and have suggested the use of peripapillary RNFL thickness to monitor patients on long-term hydroxychloroquine therapy.

---

### **Spectral-domain optical coherence tomography in central serous retinopathy**

Central serous chorioretinopathy (CSR) is characterized by serous detachment of the neurosensory retina and accumulation of serous fluid, secondary to one or more focal lesions of the RPE [Fig. 8]. It is characterized by the presence of subretinal fluid, and PED and accumulation of granular or fibrinous material may accumulate in the subretinal cavity. Chronic CSR, also known as diffuse retinal pigment epitheliopathy, is seen with a prolonged period of PED and is associated with photoreceptor atrophy and patches of irregularly pigmented RPE. SD-OCT can demonstrate shallow serous detachments that are difficult to diagnose using slit-lamp biomicroscopy or Stratus OCT. SD-OCT provides precise information about the amount and localization of subretinal fluid and RPE abnormalities in CSR. It also helps in determining a treatment plan. SD-OCT is also useful in assessing whether reattachment has occurred after treatment.

Ahlers et al. [33], have reported retinal changes during acute phase of CSR. They found that SD-OCT assists in identifying the precise location of the PED and frequently found multiple small PEDs without splitting or thickening of the RPE

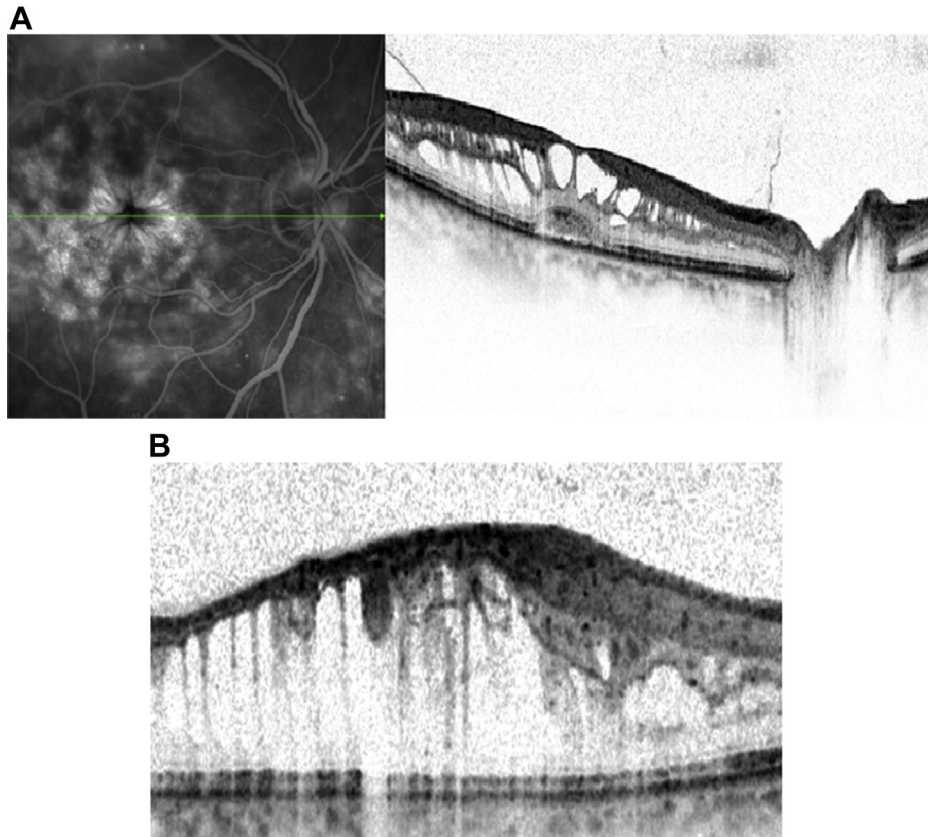


Fig. 7 – (A) Spectralis angiography with corresponding cross-sectional optical coherence tomography image of a patient with central retinal vein occlusion showing cystoid macular edema with cysts in outer plexiform and inner nuclear layer. (B) Spectralis optical coherence tomography showing cystoid macular edema in a patient with central retinal vein occlusion revealing inner retinal edema with stretched out Muller cell.

complex to be characteristic of CSR. In areas of subretinal fluid they also observed an area of hyper-reflectivity in the level of the ONL, sometimes affecting the OPL. They also found clusters of punctate subretinal deposits of hyper-reflective material in most patients. These deposits are thought to be lipophilic fragments such as residuals of rhodopsin and/or outer cone segments, present due to impaired RPE function. In a study by Ojima et al. [34], they reported that a large defect of

the outer segments in the foveal PRL correlated with poor visual acuity. In eyes with active CSR, however, the ellipsoid zone is often nondetectable in the detached retina. They also found that the restoration of ellipsoid zone in the subfoveal portion of the reattached retina is associated with relatively good visual acuity prognosis [34].

Spaide has previously reported the use of EDI OCT, in CSR. The choroid in eyes with CSR was found to be much thicker than normal. Maruko et al. [35], have reported the use of EDI-OCT to show the decrease in choroidal thickness in patients with resolved CSC treated with photodynamic therapy (PDT). Chronic CSC may be difficult to differentiate from occult choroidal neovascularization secondary to CSC.

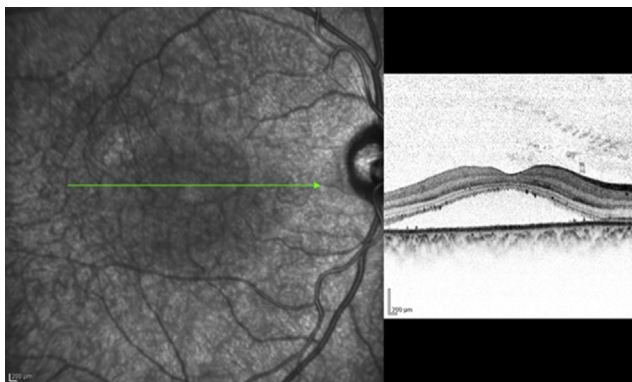


Fig. 8 – Spectralis optical coherence tomography image of a patient with central serous retinopathy. Note the foveal layers are intact with minimal disorganization.

### Spectral-domain optical coherence tomography in macular telangiectasia

One of the characteristic findings of idiopathic macular telangiectasia is cavitation of the inner retina in the foveola, which Nowilaty et al. [36], have described as a draping of the ILM across the foveola related to an underlying loss of tissue. In addition, in their series, they have reported a lack of correlation between retinal thickening on OCT and leakage on FA, cyst-like structures in the foveola and within internal retinal layers such as the inner nuclear or GCL and central intra-

retinal deposits and plaques. Similar findings have been reported by Maruko et al. [37].

### Spectral-domain optical coherence tomography in diseases of the vitreoretinal interface

Classic diseases of the vitreoretinal interface include vitreomacular traction (VMT), epiretinal membrane (ERM), and macular holes (MH). Though first described in 1865 (Hassentein), the advent of OCT has significantly enhanced our ability to visualize and follow patients with this group of disease [38].

#### Vitreomacular traction

Histopathologic analysis implicated epiretinal proliferation, with and without membrane development, in the VMT [39], which has been subsequently demonstrated *in vivo* by TD [38], and SD-OCT [40]. SD-OCT affords enhanced resolution and segmentation of the retina [6,11], where changes in PRL have been functionally correlated with vision [Fig. 9]. SD-OCT further allows for 3D documentation of VMT which can assist in surgical planning and monitoring [40]. Recently, a 2 years prospective study correlated the structural improvement of the retina, documented by SD-OCT, with recovery of visual acuity in patients following surgery for VMT. High-resolution imaging provided by SD-OCT allowed for postoperative monitoring of changes in retinal morphology. The authors reported a slower improvement in inner and outer layers of the retina as compared to surface irregularities, and a positive correlation with these changes and best-corrected visual acuity.

#### Epiretinal membrane

ERM are clinically evident in up to 6% of the population [41], and consist of myofibroblasts, astrocytes, and fibrous astrocytes [39]. Racial differences can affect the prevalence with higher rates reported in the Latino population in America (29.9%) [42], as compared to the Chinese population (39%). Idiopathic ERM's are thought to result as a consequence of posterior vitreous separation and can develop secondary to vitreous hemorrhage, inflammatory disease [43], retinal vascular disease, and both surgical and nonsurgical trauma. A recent Chinese population

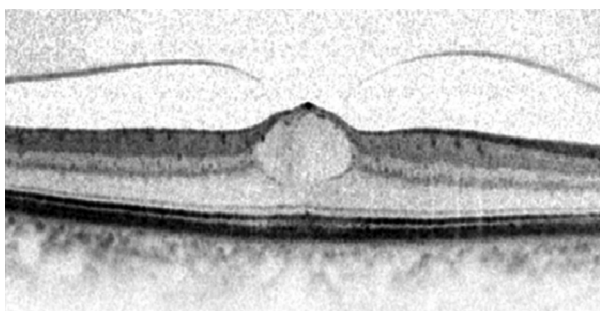


Fig. 9 – Spectralis optical coherence tomography revealing partially detached posterior hyaloid with attachment to the fovea leading to traction and cystic changes.

based study that evaluated the presence of ERM using TD-OCT revealed a prevalence of 3.0% based on fundus photography alone and 3.4% based on the combination of photography and OCT. This is the first study to document the prevalence of ERM with the use of OCT and suggests that this imaging modality may be able to demonstrate additional cases. Unfortunately, no such large population based studies are available that evaluate the prevalence of ERM using SD-OCT at this time. It is likely that a higher prevalence will be reported compared with TD-OCT, as it has been shown that SD-OCT is superior in demonstrating ERM's [44]. Further, SD-OCT is more accurate than TD-OCT in delineating epiretinal pathology from inner retinal layers. 3D analysis of SD-OCT images has further enhanced our understanding of the morphology of ERM's and their relationship with the underlying retina [45]. A recent prospective study, evaluated ultra-structural changes in the outer retina and correlated them with visual improvement in patients following membrane peeling using SD-OCT, over 3 months of follow-up. This kind of correlation can assist the surgeon in predicting and monitoring functional outcomes in patients with ERM's following membrane peeling [46].

#### Macular holes

The incidence of MH increases with age and demonstrates female predominance. MH can largely be categorized into two groups: (1) Idiopathic and (2) traumatic, with idiopathic MH [Fig. 10A and B] being five times more common than traumatic MH. Other associations including ocular (CME, neodymium-doped yttrium aluminum garnet-laser, surgery) and systemic conditions have been reported. Proposed theories on the vitreoretinal interface have been reported for both idiopathic and traumatic MHs [47]. Only few reports in the literature exist on application of OCT in traumatic MH. TD-OCT has been used to describe the morphologic features of traumatic MH [48], and to compare them with idiopathic MH [49]. It appears from the lack of literature, the greatest application of SD-OCT is in evaluation and management of idiopathic MH.

It has been previously established that SD-OCT affords greater segmentation analysis and details of the outer retina as compared to traditional TD-OCT [9,12,44]. SD-OCT has been shown to demonstrate photoreceptor outer-segment disruption and that this correlated with reduced visual acuity in patients with idiopathic MH [50]. Subsequently, independent retrospective studies evaluated the pre- and post-operative changes in SD-OCT to provide prognostic information to patients undergoing vitrectomy for idiopathic MH based on the characteristics of the disruption in inner and outer retinal segments [51]. Thus, ultra-structural retinal changes visualized by SD-OCT are useful in counseling patients on potential visual recovery following closure of idiopathic MH. Further studies are required to provide such information in the cases of traumatic MH.

#### Spectral-domain optical coherence tomography in intra-ocular tumors

Choroidal nevus is commonly found and only a small number undergo malignant transformation. While evaluating small

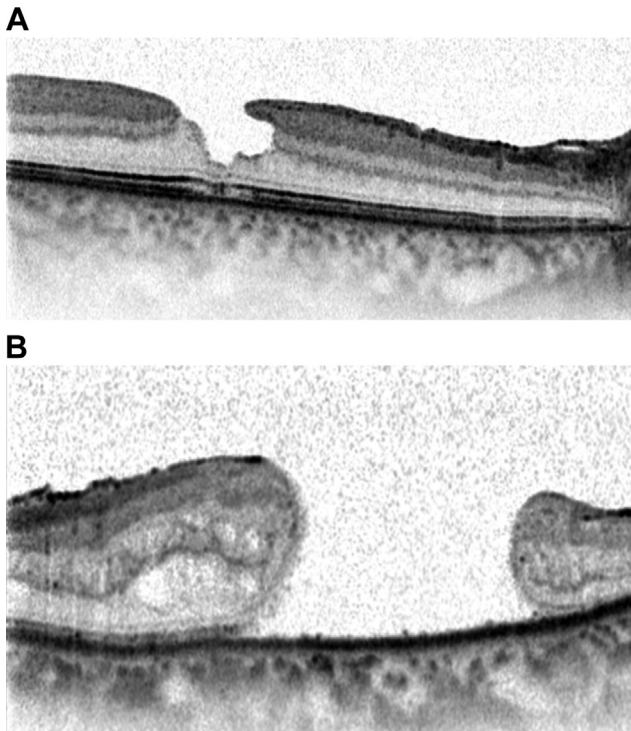


Fig. 10 – (A) Spectralis optical coherence tomography cross-sectional image of a patient with inner lamellar macular hole. There is a tractional component with an epiretinal membrane seen nasally. (B) Spectralis optical coherence tomography cross-sectional image of a full-thickness chronic macular hole. There are cystic changes in the retina with elevation of the edges of the hole by subretinal fluid.

choroidal melanocytic lesions, growth is considered as a surrogate for melanoma. In addition to quantitative features (size: Basal diameter and height) several qualitative features such as the presence of orange pigment, subretinal fluid and absence of drusen predict risk of growth of choroidal melanocytic lesions. These factors are now well established to indicate prognostic significance of the melanoma and are amenable to assessment by SD-OCT. However, due to limited tissue penetration SD-OCT does not detect significant differences in the internal characteristics of the choroidal tumors.

The presence or absence of drusen, SRF was based on an analysis of SD-OCT images centered on the melanocytic lesion,

while orange pigment was identified as focal hyper-autofluorescent spots on FAF imaging. This was studied by Singh et al. [52], and they found no statistically significant difference in detection rates of drusen, subretinal fluid, and orange pigment between ophthalmoscopic examination and SD-OCT.

Choroidal hemangioma is a vascular hamartoma that occurs sporadically, in a circumscribed isolated form, or as a diffuse choroidal angiomas. On SD-OCT, choroidal hemangioma, the mass itself is imaged with limited resolution with an area of hyper-reflectivity on its anterior surface. On SD-OCT it may appear as a dome shaped elevation of the choroid and focal hyper-plasia of the overlying RPE and retinal serous detachment [Fig. 11]. Imaging the overlying retina is useful to determine the etiology for the vision loss. The tumor may remain clinically stable or show enlargement or progressive exudation leading to CME and SRF and subretinal fibrosis which may induce vision loss. Presence of these factors usually mandates treatment. Treatment modalities may include laser, brachytherapy or more recently PDT.

SD-OCT is an important tool in depicting resolution of subretinal fluid and foveal edema following therapy. Additionally, SD-OCT can be useful in planning the treatment and prognosticating the final visual outcome following treatment for circumscribed choroidal hemangiomas. We have recently reported a case of a patient with choroidal hemangioma treated with PDT [53]. We noted resolution of intra-retinal edema, resolution of SRF, and disappearance of RPE changes on SD-OCT.

Combined hamartoma of the retina and RPE is a rare disorder diagnosed mainly in infants and young children. It could be asymptomatic or characterized by visual acuity loss, strabismus. Clinically the lesion is typically juxtapapillary or peripheral in location. The juxtapapillary lesions have variable pigmentation, are elevated, have vascular tortuosity, have vitreoretinal interface changes with ERM and lipid exudates. Peripheral lesions appear as an elevated gray ridge concentric to the ora serrata that may produce dragging of the large retinal vessels. Differential diagnosis of this lesion includes choroidal nevus and choroidal melanoma. Vitreo-retinal interface change is likely and is responsible for vision loss in some patients; it is well imaged by SD-OCT. All these findings may help with surgical intervention. On SD-OCT the lesion has been described as a hyper-reflective ERM with traction and retinal folds. Within the retina it appears as an elevated hyper-reflective mass with an underlying attenuation of the outer retina and PRL. The mass appears to be disorganized and

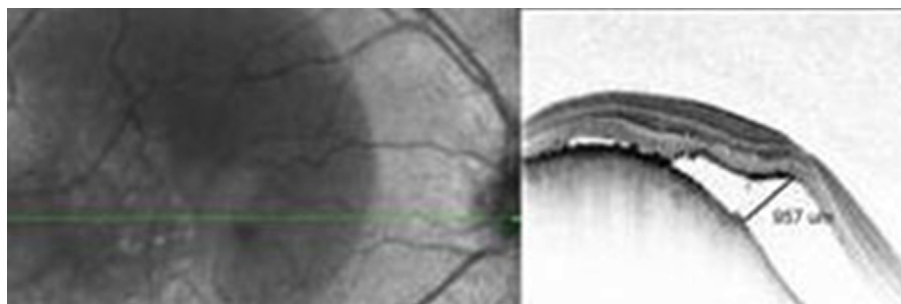


Fig. 11 – Spectralis optical coherence tomography cross-sectional image of choroidal hemangioma revealing the choroidal mass with overlying serous retinal detachment of the macula.

thick. Combined hamartomas of the retina and RPE have unique OCT characteristics highlighted with the newer-generation high-resolution instruments, which may be necessary in both diagnosis and surgical planning.

### Spectral-domain optical coherence tomography in inherited retinal disorders

Even though SD-OCT has been used in the ophthalmic community for the past decade, we are just beginning to understand its value in the evaluation of a number of inherited retinal diseases, including Stargardt's disease, Best's disease, Adult-onset foveomacular vitelliform dystrophy (AOFVD), retinitis pigmentosa, and cone dystrophy. Before any macular pathology is visible on fundus examination, SD-OCT allows us to identify the pattern and the extent of the neurosensory retinal disorganization in terms of RPE and photoreceptor cell loss in these dystrophies.

#### Stargardt's disease

Described by Stargardt in 1909, it is a bilateral symmetric maculopathy, characterized by the presence of a variable number of fish-scale shaped, yellowish, autofluorescent deposits [54]. OCT anomalies occur very early in Stargardt disease including loss of the foveal clivus, discontinuity or loss of the PRL, and retinal thinning. The retinal flecks have an appearance of hyper-reflective deposits opposed to the pigment epithelium, or rarely, further away in the ONL. Type 1 flecks are dome-shaped deposits located within the RPE and the outer segment of photoreceptors. Type 2 flecks are deposits involving the ONL as well. They are encountered in advanced or severe stages, with the loss of the PRL within the central foveal zone, ultimately leading to foveal atrophy [Fig. 12].

#### Best disease

Vitelliform macular dystrophy, also known as Best disease, was described by Friedrich Best in 1905. Most cases have a solitary lesion in the macula; others have multifocal vitelliform lesions, which are largely confined to the posterior pole [Fig. 13]. Querques et al. [55], based on SD-OCT scans, described the macular lesions as follows: (1) Previtelliform lesions, characterized by the presence of a layer between the RPE and the photoreceptor ellipsoid zone interface, corresponding to the Verhoeff membrane, which appears thicker and more reflective in the central region than the normal macula; (2) Vitelliform lesions, characterized by the yellowish material that appears as a highly reflective area, located between the hypo-reflective ONL and the hyper-reflective RPE layer. Also, focal disruption of ellipsoid zone interface over the lesion is present; (3) Pseudohypopyon lesions, characterized by two different zones-in the upper part of the lesion, SD-OCT showed an optically empty zone (hypo-reflectivity) with clumping of hyper-reflective material on the posterior retinal surface, located between the RPE and the photoreceptor ellipsoid zone interface. In the lower part of the lesion, where

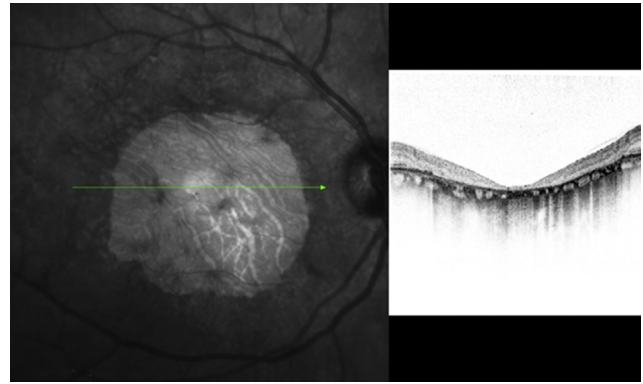


Fig. 12 – Spectralis optical coherence tomography of a patient with advanced Stargardt's disease revealing foveal atrophy with surrounding flecks.

the material is still visible, in SD-OCT showed the yellowish material that appears as a highly reflective area, located between the hypo-reflective ONL and the hyper-reflective RPE layer, comparable with the vitelliform lesion; (4) Vitelliruptive lesions, characterized by an optically empty lesion with clumping of hyper-reflective material on the posterior retinal surface, located between the RPE and the photoreceptor ellipsoid zone interface, comparable with the upper part of the pseudohypopyon; (5) Atrophic lesions, characterized by thinning of all the retinal layers and diffuse loss of the ellipsoid zone interface (complete absence of the hyper-reflective layer corresponding to the ellipsoid zone interface) within the macular area, with enhanced RPE reflectivity; (6) Fibrotic lesions, characterized by a prominent, highly hyper-reflective thickening at RPE level, inducing marked anterior bulging, accompanied by thinning of the sensory retina and diffuse loss of the ellipsoid zone interface above it.

#### Adult-onset foveomacular vitelliform dystrophy adult-onset foveomacular vitelliform dystrophy

AOFVD is a relatively uncommon macular disease first described by Gass [56], in 1974. Fundus examination shows a

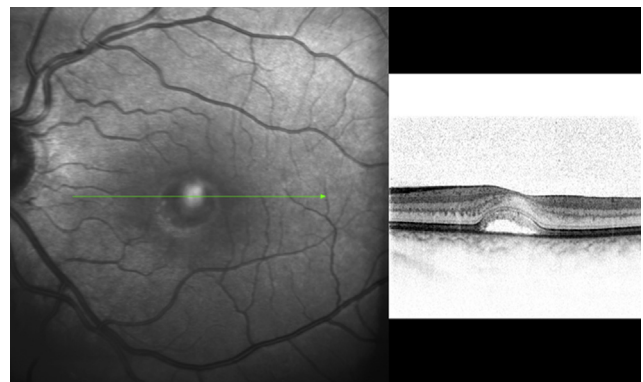


Fig. 13 – Spectralis optical coherence tomography of a patient with Best disease showing buildup of lipofuscin, between the outer retina and the retinal pigment epithelium.

subretinal oval or round elevated deposit of yellowish vitelliform material located in the macular area [Fig. 14]. The exact location of the vitelliform material in AOFVD has not been fully elucidated by previous clinical or histological descriptions. Puche et al. [57], with the help of SD-OCT showed the vitelliform material as a highly reflective dome-shaped lesion located between the PRL and RPE. In their study, the vitelliform material appeared homogeneous in 14/60 eyes and heterogeneous in 36/60 eyes. An optically empty zone between the PRL and the material, and/or the RPE layer was observed within the hyper-reflective vitelliform lesion in 29/60 eyes. The ellipsoid zone interface appeared highly reflective, showing a shell-like aspect all around the vitelliform material in 27/60 eyes. The RPE was found to be irregular with hyper-reflective mottling with discrete RPE detachments seen in 29/60 eyes.

### Retinitis pigmentosa

RP is a group of inherited disorders characterized by progressive peripheral vision loss and night vision difficulties that can lead to central vision loss by progressive degeneration of the photoreceptors. OCT can identify vitreoretinal abnormalities associated with RP that often contribute to the deterioration of visual acuity in these patients [58]. In RP, SD-OCT reveals loss

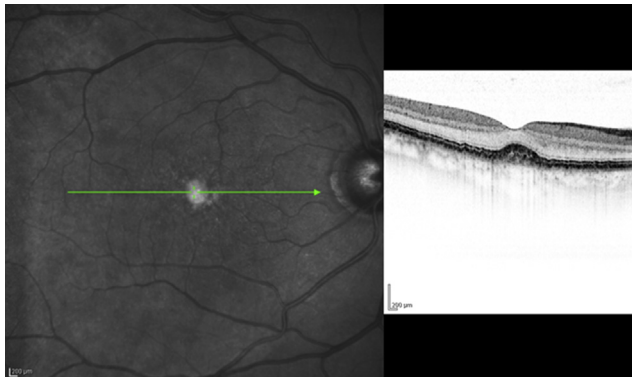


Fig. 14 – Spectralis optical coherence tomography of a patient with adult-onset foveo-macular vitelliform dystrophy revealing accumulation of vitelliform material between the and neuro-sensory retina.

of the ellipsoid zone at one or more peripheral locations from early stages followed by overall marked reduction of the total retinal thickness. Aizawa et al. [59], showed ellipsoid zone junction to be absent in 5–31% of the cases. Triolo et al. [58], found that the ellipsoid zone junction was either absent or disrupted within the foveal region in 13.6% and 47.7% of cases, respectively. CME macular edema, if present, is very easily seen on SD-OCT even though it doesn't leak on fluorescence angiography. ERM is seen as a hyper-reflective membrane on the surface of the retina [Fig. 15].

### Cone dystrophy

The progressive cone dystrophies represent a heterogeneous group of diseases with onset in teenage years or later adult life [60]. Many patients develop rod photoreceptor involvement in later life, leading to considerable overlap between progressive cone and cone-rod dystrophies. Cone dystrophies are diagnosed by an abnormal or nonrecordable photopic electroretinogram (ERG) and a normal or near-normal rod-isolated ERG, whereas peripheral visual fields remain normal. SD-OCT finding may be recognized before any pathology becomes evident on fundus examination. The loss of photoreceptors predominates in the foveolar or perifoveolar zones giving rise to the classic bull's eye pattern. Absence of ellipsoid zone junction and RPE gives rise to the hyper-reflective signal of the choroid.

### Retinoschisis

Degenerative or acquired retinoschisis (RS) is a split in the neurosensory retina, which is usually asymptomatic, rarely progressive, but often presents a diagnostic dilemma on routine dilated funduscopy. Inner and outer schisis cavity appeared to be separated by the OPL [61]. The irregularity of the inner surface of the attached outer leaf was identified in all RS patients [61].

### Spectral-domain optical coherence tomography in retinopathy of prematurity

Retinopathy of prematurity (ROP) is a multifactorial vascular disease and timely treatment of ROP is important to prevent

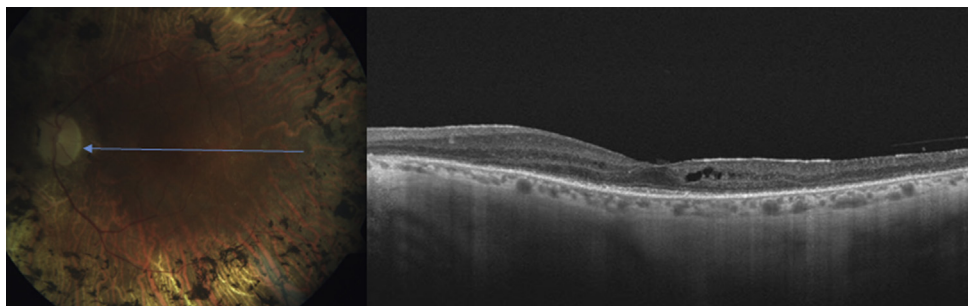


Fig. 15 – Spectralis optical coherence tomography of a patient with retinitis pigmentosa with associated cystoid macular edema and external limiting membrane.

disease progression and improve visual outcomes. SD-OCT is also been tried to assess the macular and retinal changes in the premature retina, allowing detection of subclinical anatomic changes in infants, although data on its use in ROP screening are limited. Maldonado et al. [62], have reported CME as a common finding in their cohort of premature babies, which did not differ by race and when present, was almost always bilateral. Increased severity of CME, identified by, was associated with subsequent laser treatment, with plus disease and with higher ROP stage. Chavala [63], and coworkers have reported the use of hand held SD-OCT for the assessment of retina in ROP babies, which can be done in neonatal intensive care settings. Wu et al. [64], reported retention of the layer of retinal ganglion cells, IPL, and inner nuclear layer in ROP babies who needed treatment in form of laser or cryotherapy.

### Miscellaneous

Although OCT has been widely employed in retinal diseases, it is also important to mention the application of OCT in choroidal diseases and in myopia.

In patients with high axial myopia, there can be associated degenerative changes in the sclera, choroid, and retina involving the macula [65]. Common macular changes in highly myopic eyes are maculoschisis, posterior vitreous detachment, disruption of the photoreceptor ellipsoid zone interface, ERMs, defects in Bruch's membrane, clumping of the RPE, vitreofoveal adhesion, and MH [65]. Majorities of these changes are structural and can be clearly delineated using different OCT techniques. Changes like disruption of the ellipsoid zone and ERM formation can have a functional impact by negatively affecting the visual acuity [65].

In the past, insight into the majority of choroidal diseases has been through histological postmortem studies or invasive methods such as indocyanine green angiography and FA [66]. However, with the advent of EDI-OCT [66] and more recently swept source OCT (SS-OCT) [67], we can obtain *in vivo* 3D anatomical information about the choroid. SS-OCT employs a longer wavelength (1080 nm) which enables it to have a deeper penetration of ocular tissues beyond the photoreceptor and RPE layers, allowing visualization of choroid–scleral junction.

### Conclusion

SD-OCT has evolved over a decade as one of the most important diagnostic tools in ophthalmology. It not only helps us in diagnosing the retinal and choroidal pathologies but also guides us in monitoring the response to treatment. Now with advanced OCT (EDI- and SS-OCT) better deeper visualization is possible. There are opportunities for new directions in research and clinical practice with ongoing evolution of OCT technology and easier availability to the clinicians and researchers.

### Source of support

Nil.

### Conflicts of interest

None declared.

### REFERENCES

- [1] Huang D, Swanson EA, Lin CP, Schuman JS, Stinson WG, Chang W, et al. Optical coherence tomography. *Science* 1991;254:1178–81.
- [2] Puliafito CA, Hee MR, Lin CP, Reichel E, Schuman JS, Duker JS, et al. Imaging of macular diseases with optical coherence tomography. *Ophthalmology* 1995;102:217–29.
- [3] Hee MR, Puliafito CA, Wong C, Duker JS, Reichel E, Rutledge B, et al. Quantitative assessment of macular edema with optical coherence tomography. *Arch Ophthalmol* 1995;113:1019–29.
- [4] Schaudig UH, Glaefke C, Scholz F, Richard G. Optical coherence tomography for retinal thickness measurement in diabetic patients without clinically significant macular edema. *Ophthalmic Surg Lasers* 2000;31:182–6.
- [5] Shahidi M, Ogura Y, Blair NP, Rusin MM, Zeimer R. Retinal thickness analysis for quantitative assessment of diabetic macular edema. *Arch Ophthalmol* 1991;109:1115–9.
- [6] Wojtkowski M, Srinivasan V, Fujimoto JG, Ko T, Schuman JS, Kowalczyk A, et al. Three-dimensional retinal imaging with high-speed ultrahigh-resolution optical coherence tomography. *Ophthalmology* 2005;112:1734–46.
- [7] Alam S, Zawadzki RJ, Choi S, Gerth C, Park SS, Morse L, et al. Clinical application of rapid serial Fourier-domain optical coherence tomography for macular imaging. *Ophthalmology* 2006;113:1425–31.
- [8] Srinivasan VJ, Wojtkowski M, Witkin AJ, Duker JS, Ko TH, Carvalho M, et al. High-definition and 3-dimensional imaging of macular pathologies with high-speed ultrahigh-resolution optical coherence tomography. *Ophthalmology* 2006;113(2054):e1–14.
- [9] Nassif N, Cense B, Park B, Pierce M, Yun S, Bouma B, et al. *In vivo* high-resolution video-rate spectral-domain optical coherence tomography of the human retina and optic nerve. *Opt Express* 2004;12:367–76.
- [10] Han IC, Jaffe GJ. Evaluation of artifacts associated with macular spectral-domain optical coherence tomography. *Ophthalmology* 2010;117. 1177–1189.e4.
- [11] Grover S, Murthy RK, Brar VS, Chalam KV. Normative data for macular thickness by high-definition spectral-domain optical coherence tomography (spectralis). *Am J Ophthalmol* 2009;148:266–71.
- [12] Grover S, Murthy RK, Brar VS, Chalam KV. Comparison of retinal thickness in normal eyes using Stratus and Spectralis optical coherence tomography. *Invest Ophthalmol Vis Sci* 2010;51:2644–7.
- [13] Chung H, Park B, Shin HJ, Kim HC. Correlation of fundus autofluorescence with spectral-domain optical coherence tomography and vision in diabetic macular edema. *Ophthalmology* 2012;119:1056–65.
- [14] Paunescu LA, Schuman JS, Price LL, Stark PC, Beaton S, Ishikawa H, et al. Reproducibility of nerve fiber thickness, macular thickness, and optic nerve head measurements using Stratus OCT. *Invest Ophthalmol Vis Sci* 2004;45:1716–24.
- [15] Polito A, Del Borrello M, Isola M, Zemella N, Bandello F. Repeatability and reproducibility of fast macular thickness mapping with stratus optical coherence tomography. *Arch Ophthalmol* 2005;123:1330–7.
- [16] Gürses-Ozden R, Teng C, Vessani R, Zafar S, Liebmann JM, Ritch R. Macular and retinal nerve fiber layer thickness

- measurement reproducibility using optical coherence tomography (OCT-3). *J Glaucoma* 2004;13:238–44.
- [17] Muscat S, Parks S, Kemp E, Keating D. Repeatability and reproducibility of macular thickness measurements with the Humphrey OCT system. *Invest Ophthalmol Vis Sci* 2002;43:490–5.
- [18] Joeres S, Tsong JW, Updike PG, Collins AT, Dustin L, Walsh AC, et al. Reproducibility of quantitative optical coherence tomography subanalysis in neovascular age-related macular degeneration. *Invest Ophthalmol Vis Sci* 2007;48:4300–7.
- [19] Leung CK, Cheung CY, Weinreb RN, Lee G, Lin D, Pang CP, et al. Comparison of macular thickness measurements between time domain and spectral domain optical coherence tomography. *Invest Ophthalmol Vis Sci* 2008;49:4893–7.
- [20] Costa-Cunha LV, Cunha LP, Malta RF, Monteiro ML. Comparison of Fourier-domain and time-domain optical coherence tomography in the detection of band atrophy of the optic nerve. *Am J Ophthalmol* 2009;147: 56–63.e2.
- [21] Foroghian F, Cukras C, Meyerle CB, Chew EY, Wong WT. Evaluation of time domain and spectral domain optical coherence tomography in the measurement of diabetic macular edema. *Invest Ophthalmol Vis Sci* 2008;49:4290–6.
- [22] Otani T, Kishi S. Correlation between optical coherence tomography and fluorescein angiography findings in diabetic macular edema. *Ophthalmology* 2007;114:104–7.
- [23] Maheshwary AS, Oster SF, Yuson RM, Cheng L, Mojana F, Freeman WR. The association between percent disruption of the photoreceptor inner segment-outer segment junction and visual acuity in diabetic macular edema. *Am J Ophthalmol* 2010;150: 63–67.e1.
- [24] Querques G, Canoui-Poitrine F, Coscas F, Massamba N, Querques L, Mimoun G, et al. Analysis of progression of reticular pseudodrusen by spectral domain–optical coherence tomography. *Invest Ophthalmol Vis Sci* 2012;53:1264–8.
- [25] Schuman SG, Koreishi AF, Farsiu S, Jung SH, Izatt JA, Toth CA. Photoreceptor layer thinning over drusen in eyes with age-related macular degeneration imaged *in vivo* with spectral-domain optical coherence tomography. *Ophthalmology* 2009;116: 488–496.e2.
- [26] Fleckenstein M, Charbel Issa P, Helb HM, Schmitz-Valckenberg S, Finger RP, Scholl HP, et al. High-resolution spectral domain-OCT imaging in geographic atrophy associated with age-related macular degeneration. *Invest Ophthalmol Vis Sci* 2008;49:4137–44.
- [27] Margolis R, Spaide RF. A pilot study of enhanced depth imaging optical coherence tomography of the choroid in normal eyes. *Am J Ophthalmol* 2009;147:811–5.
- [28] Khurana RN, Dupas B, Bressler NM. Agreement of time-domain and spectral-domain optical coherence tomography with fluorescein leakage from choroidal neovascularization. *Ophthalmology* 2010;117:1376–80.
- [29] Framme C, Panagakis G, Birngruber R. Effects on choroidal neovascularization after anti-VEGF Upload using intravitreal ranibizumab, as determined by spectral domain-optical coherence tomography. *Invest Ophthalmol Vis Sci* 2010;51:1671–6.
- [30] Ota M, Tsujikawa A, Murakami T, Kita M, Miyamoto K, Sakamoto A, et al. Association between integrity of foveal photoreceptor layer and visual acuity in branch retinal vein occlusion. *Br J Ophthalmol* 2007;91:1644–9.
- [31] Ota M, Nishijima K, Sakamoto A, Murakami T, Takayama K, Horii T, et al. Optical coherence tomographic evaluation of foveal hard exudates in patients with diabetic maculopathy accompanying macular detachment. *Ophthalmology* 2010;117:1996–2002.
- [32] Chen E, Brown DM, Benz MS, Fish RH, Wong TP, Kim RY, et al. Spectral domain optical coherence tomography as an effective screening test for hydroxychloroquine retinopathy (the “flying saucer” sign). *Clin Ophthalmol* 2010;4:1151–8.
- [33] Ahlers C, Geitzenauer W, Stock G, Golbaz I, Schmidt-Erfurth U, Prunte C. Alterations of intraretinal layers in acute central serous chorioretinopathy. *Acta Ophthalmol* 2009;87:511–6.
- [34] Ojima Y, Hangai M, Sasahara M, Gotoh N, Inoue R, Yasuno Y, et al. Three-dimensional imaging of the foveal photoreceptor layer in central serous chorioretinopathy using high-speed optical coherence tomography. *Ophthalmology* 2007;114:2197–207.
- [35] Maruko I, Iida T, Sugano Y, Furuta M, Sekiryu T. One-year choroidal thickness results after photodynamic therapy for central serous chorioretinopathy. *Retina* 2011;31:1921–7.
- [36] Nowilaty SR, Al-Shamsi HN, Al-Khars W. Idiopathic juxtafoveal retinal telangiectasis: a current review. *Middle East Afr J Ophthalmol* 2010;17:224–41.
- [37] Maruko I, Iida T, Sugano Y, Ojima A, Oyamada H, Sekiryu T. Demographic features of idiopathic macular telangiectasia in Japanese patients. *Jpn J Ophthalmol* 2012;56:152–8.
- [38] Mirza RG, Johnson MW, Jampol LM. Optical coherence tomography use in evaluation of the vitreoretinal interface: a review. *Surv Ophthalmol* 2007;52:397–421.
- [39] Zhao F, Gandorfer A, Haritoglou C, Scheler R, Schaumberger MM, Kampik A, et al. Epiretinal cell proliferation in macular pucker and vitreomacular traction syndrome: analysis of flat-mounted internal limiting membrane specimens. *Retina* 2013;33:77–88.
- [40] Wong IY, Koizumi H, Lai WW. Enhanced depth imaging optical coherence tomography. *Ophthalmic Surg Lasers Imaging* 2011;(42 suppl):S75–84.
- [41] McCarty DJ, Mukesh BN, Chikani V, Wang JJ, Mitchell P, Taylor HR, et al. Prevalence and associations of epiretinal membranes in the visual impairment project. *Am J Ophthalmol* 2005;140:288–94.
- [42] Ng CH, Cheung N, Wang JJ, Islam AF, Kawasaki R, Meuer SM, et al. Prevalence and risk factors for epiretinal membranes in a multi-ethnic United States population. *Ophthalmology* 2011;118:694–9.
- [43] Bringmann A, Wiedemann P. Involvement of Müller glial cells in epiretinal membrane formation. *Graefes Arch Clin Exp Ophthalmol* 2009;247:865–83.
- [44] Nigam N, Bartsch DU, Cheng L, Brar M, Yuson RM, Kozak I, et al. Spectral domain optical coherence tomography for imaging ERM, retinal edema, and vitreomacular interface. *Retina* 2010;30:246–53.
- [45] Legarreta JE, Gregori G, Knighton RW, Punjabi OS, Lalwani GA, Puliafito CA. Three-dimensional spectral-domain optical coherence tomography images of the retina in the presence of epiretinal membranes. *Am J Ophthalmol* 2008;145:1023–30.
- [46] Inoue M, Morita S, Watanabe Y, Kaneko T, Yamane S, Kobayashi S, et al. Inner segment/outer segment junction assessed by spectral-domain optical coherence tomography in patients with idiopathic epiretinal membrane. *Am J Ophthalmol* 2010;150:834–9.
- [47] Besirli CG, Johnson MW. Traction-induced foveal damage predisposes eyes with pre-existing posterior vitreous detachment to idiopathic macular hole formation. *Eye (Lond)* 2012;26:792–5.
- [48] Arevalo JF, Sanchez JG, Costa RA, Farah ME, Berrocal MH, Graue-Wiechers F, et al. Optical coherence tomography characteristics of full-thickness traumatic macular holes. *Eye (Lond)* 2008;22:1436–41.
- [49] Huang J, Liu X, Wu Z, Sadda S. Comparison of full-thickness traumatic macular holes and idiopathic macular holes by

- optical coherence tomography. *Graefes Arch Clin Exp Ophthalmol* 2010;248:1071–5.
- [50] Chang E, Garg P, Capone Jr A. Outcomes and predictive factors in bilateral macular holes. *Ophthalmology* 2013;120:1814–9.
- [51] Chalam KV, Murthy RK, Gupta SK, Brar VS, Grover S. Foveal structure defined by spectral domain optical coherence tomography correlates with visual function after macular hole surgery. *Eur J Ophthalmol* 2010;20:572–7.
- [52] Sayanagi K, Pelayes DE, Kaiser PK, Singh AD. 3D Spectral domain optical coherence tomography findings in choroidal tumors. *Eur J Ophthalmol* 2011;21:271–5.
- [53] Chalam KV, Murthy RK, Gupta SK, Brar VS. Spectral domain optical coherence tomography guided photodynamic therapy for choroidal hemangioma: a case report. *Cases J* 2009;2:8778.
- [54] Fujinami K, Lois N, Mukherjee R, McBain VA, Tsunoda K, Tsubota K, et al. A longitudinal study of Stargardt disease: quantitative assessment of fundus autofluorescence, progression, and genotype correlations. *Invest Ophthalmol Vis Sci* 2013;54:8181–90.
- [55] Querques G, Regenbogen M, Quijano C, Delphin N, Soubrane G, Souied EH. High-definition optical coherence tomography features in vitelliform macular dystrophy. *Am J Ophthalmol* 2008;146:501–7.
- [56] Gass JD. A clinicopathologic study of a peculiar foveomacular dystrophy. *Trans Am Ophthalmol Soc* 1974;72:139–56.
- [57] Puche N, Querques G, Benhamou N, Tick S, Mimoun G, Martinelli D, et al. High-resolution spectral domain optical coherence tomography features in adult onset foveomacular vitelliform dystrophy. *Br J Ophthalmol* 2010;94:1190–6.
- [58] Triolo G, Pierro L, Parodi MB, De Benedetto U, Gagliardi M, Manitto MP, et al. Spectral domain optical coherence tomography findings in patients with retinitis pigmentosa. *Ophthalmic Res* 2013;50:160–4.
- [59] Aizawa S, Mitamura Y, Baba T, Hagiwara A, Ogata K, Yamamoto S. Correlation between visual function and photoreceptor inner/outer segment junction in patients with retinitis pigmentosa. *Eye (Lond)* 2009;23:304–8.
- [60] Michaelides M, Hardcastle AJ, Hunt DM, Moore AT. Progressive cone and cone-rod dystrophies: phenotypes and underlying molecular genetic basis. *Invest Ophthalmol* 2006;51:232–58.
- [61] Yeoh J, Rahman W, Chen FK, da Cruz L. Use of spectral-domain optical coherence tomography to differentiate acquired retinoschisis from retinal detachment in difficult cases. *Retina* 2012;32:1574–80.
- [62] Maldonado RS, O'Connell R, Ascher SB, Sarin N, Freedman SF, Wallace DK, et al. Spectral-domain optical coherence tomographic assessment of severity of cystoid macular edema in retinopathy of prematurity. *Arch Ophthalmol* 2012;130:569–78.
- [63] Chavala SH, Farsiu S, Maldonado R, Wallace DK, Freedman SF, Toth CA. Insights into advanced retinopathy of prematurity using handheld spectral domain optical coherence tomography imaging. *Ophthalmology* 2009;116:2448–56.
- [64] Wu WC, Lin RI, Shih CP, Wang NK, Chen YP, Chao AN, et al. Visual acuity, optical components, and macular abnormalities in patients with a history of retinopathy of prematurity. *Ophthalmology* 2012;119:1907–16.
- [65] You QS, Peng XY, Xu L, Chen CX, Wang YX, Jonas JB. Myopic maculopathy imaged by optical coherence tomography: the Beijing Eye Study. *Ophthalmology* 2014;121:220–4.
- [66] Lavers H, Zambarakji H. Enhanced depth imaging-OCT of the choroid: a review of the current literature. *Graefes Arch Clin Exp Ophthalmol* 2014;252:1871–83.
- [67] Mrejen S, Spaide RF. Optical coherence tomography: imaging of the choroid and beyond. *Surv Ophthalmol* 2013;58:387–429.